Can historical data predict population responses to climate change experiments?

Andrew R. Kleinhesselink[*a], Peter B. Adler[a] and Andrew Tredennick[a]

[a]Department of Wildland Resources and the Ecology Center, Utah State University, Logan, Utah

Last compile: December 18, 2016

Keywords: Climate change, demographic models, rain-out shelter.

Running title: Predicting climate response

Article type: Letter

Authorship statement: ARK and PBA designed the experiment and supervised data collection. AT helped with the data analysis.

---
[*]Corresponding author. Department of Wildland Resources and the Ecology Center, Utah State University, Logan, Utah Email: arklein@aggiemail.usu.edu

Summary

1. Climate is an important driver of population ecology however there have been few tests of whether observational data that links population performance with climate variation can be used to predict the responses of populations to experimentally imposed climate conditions.

2. Using longterm historical observational data from a sagebrush steppe plant community, previous research has reported a wide variety of climate effects on four dominant plant species. We tested whether statistical models based on these observational data could be used to predict how these species respond to a five year drought and irrigation experiment conducted from 2011 to 2016.

    item We established sixteen new plots at the same field cite as the original historical data and assigned each to either drought or irrigation treatments imposed using rainfall shelters and automatic sprinklers. The original plots were also monitored and served as ambient climate controls. In order to describe the demographic effects of the climate manipulations, we used all data, observational and experimental, to fit a set of statistical models describing each species survival, growth and recruitment in response to local competitive interactions and the effects of the climate manipulation experiment. Next we fit another set of models to only the observational data that used seasonal soil moisture covariates to describe annual variation in the vital rates. Finally, we used the observation-based models to predict the effects of the experimental treatments on each species vital rates. We also used an individual based population model to predict one year ahead changes in population size in the experimental plots.

3. The experimental drought and irrigation treatments successfully lowered and increased soil moisture respectively. Over the course of the experiment, average plot cover of *Hesperostipa comata* and *Pseudoroegneria spicata* declined, while cover of *Poa secunda* showed a trend towards increase in the irrigated plots. At the level of individual vital rates, experimental drought reduced growth of *Hesperostipa comata* and growth and survival of *Poa secunda*. Drought increased, while irrigation decreased, growth of the shrub *Artemisia tripartita*.

4. Vital rate models fit to the observational data correctly predicted significant increases in X and X and significant decreaes in X and X. However, the historical models predicted significant

changes in X X and X that were not observed in the experiment. Moreover, the experiment led to a significant change in X that was not predicted by the historical data.

5. Our individual based population model more accurately predicted changes in the population growth rates of in the experimental plots than a model without climate effects. However for the other X species predictions made from the climate model were less accurate than models without climate.

6. *Synthesis*: Out of all four species examined, climate covariates only appeared to increase our predictive accuracy for one species: *Hesperostipa comata*. In general the relatively weak responses to the experimental treatments agrees with the low explanatory power of climate covariates in explaining the vital rates and population dynamics of these species in this system. The highly variable environment and water limited conditions may select for species with a conservative non-responsive strategy to variation in climate both natural and experimentally imposed.

Introduction

Climate is widely considered one of the most powerful external forces driving changes in species abundance across space and time (Teller et al., 2016). The effects of climate on populations and ecosystems are most apparent at the largest scales in space and time: climate determines the distribution of ecosystems, treelines and the the range limits of many species (), while the recent historical and the paleoecological record shows that long-term climate change leads to changes in species range limits (??). Understanding and predicting the effects of climate on populations is an increasingly important goal if we are to understand and predict the effects of climate change on earth's ecosystems.

Unfortunately, for many species it is difficult to determine how annual climate variation affects populations and demographic rates (Teller et al., 2016; ?). Observational data on species performance across years with varying climate can provide some information on how climate might affect population abundance (??). However, many years of data are needed to reliably detect climate effects, especially when annual variation in demographic rates is high (Teller et al., 2016; ?). Generating predictions from observational historical data for the future novel conditions created by climate change is fraught with risk. Climate change will not only change mean annual temperature

and precipitation, but also affect annual variation in these measures, and possibly the covariance between them (). Models based on the historical response of populations to annual climate variation, will therefore be extrapolating beyond the range of observed climate variation when they are used to generate predictions in the future (). If models fit to historical data can be used to accurately predict the effects of experimental climate manipulations, especially manipulations that generate extreme variation in climate, it would be strong confirmation that the climate effects they describe are real and will hold in the future **?**.

Many plant species occur across a wide range of climates and individual plants in many environments must tolerate large fluctuations in seasonal temperature and soil moisture. Unlike most animals, plants must endure these conditions in place and often become dormant in less optimal seasons . At first pass, these observation would seem to indicate that annual variation in climate should have little effect on plant population performance.

Nevertheless, there is abundant evidence that plant performance shows high year to year variation, both at the level of individual growth, survival and reproduction and in terms of total population abundancend often this variation c. In many regions interannual variation in precipitation can be directly linked to variation in net primary productivity (**??**). The growth rates of trees are also often tightly linked to annual precipitation, so much so that annual growth rings in their stems can serve as accurate records of historical climate thousands of years before the present (**?**). Likewise, many smaller shrub and sub-shrub species show strong variation in growth in response to climate that is recorded in their tissues (**??**). Among annual plants in desert ecosystems, germination and reproductive output is tightly linked to interannual precipitation variation (**?**).

Linking annual climate variation to demographic performance in plants is a high priority for building population models for plants that can predict their future response to climate change (**??**). However, despite the clear signs that climate drives net primary productivity at the ecosystem level and the variation in individual growth rate in trees and other woody species, as well as the germination and fecundity of annual plants, there are few studies that have connected the effects of interannual climate variation to population models for plants, and fewer still that have tested whether these population models can be used to accurately predict the future responses of plants to short term climate variation. Adler et al. (**?**) showed that population models based on historically observed correlations between plant population growth rates and precipitation did

4

have some predictive power in describing species response to a short-term climate manipulation in a North American grassland. Three species showed responses to experimentally imposed drought and irrigation that were well predicted by population models fitted to historical observations. However, another three species, showed responses to the experimental conditions that were not well predicted by historical observations. The authors suggested that limited replication in the historical data for two of these species and changing competitive conditions in the community may have led to the poor predictions.

The demography and competitive interactions between three dominant grass species and a dominant shrub species at in a sagebrush steppe plant community at the US Sheep Experiment Station near Dubois, Idaho have been described in at least X different studies since 2005. X of these studies report significant effects of historical climate variation on the vital rates and overall population growth of these species. Both precipitation and temperature have been shown to have strong species-specific effects on this system. Although past studies used different statistical models and methods for variable selection they indicate X. This well-studied system offers the ideal opportunity to test whether statistical associations between annual climate variation and plant demography in long-term observational data can be used to predict the future responses of plant populations to climate change.

In this study, we report how the four dominant plant species at the USSES responded to a five year drought and irrigation experiment and use the results to address two research questions: first, how much do the growth, recruitment and survival of our target species differ between the precipitation manipulation treatments? If our experiment does affect species vital rates we interpret that as strong evidence that variation in precipitation should have an effect on populations. Second, we test whether statistical models parameterized from observational data only can accurately predict each species response to the experimental precipitation manipulation? If models based on observational effectively capture the effects of climate on species performance, they should also predict the effects of precipitation treatments in the experiment.

Methods

Study site and data set description

The U.S. Sheep Experiment Station (USSES) is located 9.6 km north of Dubois, Idaho (44.2°N, 112.1°W), 1500 m above sea level. During the period of data collection (1926 1957), mean annual precipitation was 270 mm and mean temperatures ranged from -8°C (January) to 21°C (July). The vegetation is dominated by a shrub, *Artemisia tripartita*, and three perennial C3 grasses: *Pseudoroegneria spicata*, *Hesperostipa comata*, and *Poa secunda*. These dominant species account for over 70% of basal cover and 60% of canopy cover at this site.

Scientists at the USSES established 26 1-m^2 quadrats between 1926 and 1932. Eighteen quadrats were distributed among four ungrazed exclosures, and eight were distributed in two paddocks grazed at medium intensity spring through fall. All quadrats were located on similar topography and soils. In most years until 1957, all individual plants in each quadrat were mapped using a pantograph (Blaisdell 1958). The historical data set is public and available online (Zachmann et al., 2010). In 2007, we located 14 of the original quadrats, all of which are inside permanent livestock exclosures, and resumed annual mapped censusing using the traditional pantograph method. Daily temperature and precipitation has been monitored throughout this period at a climate station located at the USSES headquarters (station id: GHCND:USC00102707) which located within 2 km of the research plots. We downloaded daily and monthly tmin, tmax, and precipitation data from the National Climate Data Centers online database.

We extracted data on survival, growth, and recruitment from the mapped quadrats based on plants' spatial locations. Our approach tracks genets representing individual plants. For the shrub, each genet is associated with the basal position of a stem. For the bunchgrasses, each genet represents a spatially distinct polygon in the mapped quadrat. These genets may fragment and/or coalesce over time. Each mapped polygon is classified as a surviving genet or a new recruit based on its spatial location relative to genets present in previous years (Lauenroth and Adler, 2008). We modeled vital rates using data from 21 year-to-year transitions between 1929 and 1957, and four year-to-year transitions from 2007 to 2011.

Precipitation experiment

In spring 2011, we selected locations for an additional 16 quadrats for the precipitation experiment. We located these in a large exclosure containing six of the historical permanent quadrats. We avoided plots falling on hill slopes, areas with greater than 20% bare rock, or with over 10% cover of the woody shrubs *Purshia tridentata* or *Amelanchier utahensis*. New plots were established in pairs, and one plot per pair was randomly assigned to either the precipitation reduction or the precipitation addition treatment. We mapped the quadrats in June, 2011 and then built the rainfall shelters and set-up the irrigation systems in the fall of 2011. We used a rain-out shelter and automatic irrigation design described in (**??**). Each rain-out shelter covered an area of 2.5 by 2 m and consisted of transparent acrylic shingles held up over the plot to channel 50% of incoming rainfall off of the plot and into 75 l reservoirs. The collected water was pumped out of reservoirs and sprayed onto paired irrigation treatment plots. Pumping was initiated automatically with float switches that were triggered when water levels in the reservoirs were approximately 20 l, or equivalently irrigation was triggered once for every 6 mm of rainfall collected. We disconnected the irrigation pumps in late fall each year and re-connected them in April. The drought shelters remained in place throughout the year.

We monitored soil moisture and air temperature in four of the precipitation experiment plot pairs using Decagon Devices (Pulman Washington) 5TM and EC-5 soil moisture sensors and 5TE temperature sensors. We installed two soil moisture sensors in each monitored plot at 5 cm and two at 25 cm deep in the soil. Air temperature was measured underneath the roofing of the shelter at 30 cm above ground. For each pair of manipulated plots, we also installed sensors in a nearby area to measure ambient rainfall and temperature. Data were logged automatically every four hours. We augmented automatic monitoring of the climate in these plots with by taking direct measurements of soil moisture with a handheld EC-5 soil moisture sensor around each plot at X different times in the spring and summer between 2012 and 2016.

We conducted a simple statistical to determine the net effect of the experimental treatments on cover in the experiment. First we calculated the log change in cover for each of the four focal species in each quadrat from from the start of the experiment in spring prior to manipulation, to the last year of the experiment. Log change in cover was defined as , $log(Cover_{2016}/Cover_{2011})$

where $Cover_{2016}$ is the cover of each species in 2011 and $Cover_{2015}$ is cover in 2011. We tested for the effect of precipitation treatment on this measure with a linear model in R. We considered the precipitation treatment effects to be significant when??.

Soil moisture modeling

We expected that our precipitation manipulation experiment would affect plants by altering available soil moisture during the growing season. Because we do not have direct soil moisture measures for each year of observed plant cover in the historical record, we used the SOILWAT soil moisture model to estimate daily soil moisture at the USSES from 1925 to the present (**?**). We used an enhanced version of soilwat that has recently been developed for use in semi-arid shrubland ecosystems (**?**). SOILWAT uses daily weather data, ecosystem specific vegetation properties and site specific soil properties to estimate water balance processes. SOILWAT specifically estimates rainfall interception by vegetation, evaporation of intercepted water, snow melt and snow redistribution, infiltration into the soil, percolation through the soil, bare-soil evaporation, transpiration from each soil layer, and drainage. We parameterized SOILWAT with the generic sagebrush steppe vegetation parameters and site specific soil texture and bulk density data. We used daily weather data collected at the USSES from 1925 until the present as weather forcing data for the SOILWAT predictions.

We averaged daily soil moisture predictions from SOILWAT from upper 40 cm of soil and then aggregated these seasonally to serve as the covariates in the vital rate regressions for each species. In order to predict species' performance in the experimental plots we took the raw SOILWAT predictions for the ambient conditions for each day during the experimental period and then adjusted these up or down using coefficients from a linear model fit to the changes in soil moisture directly observed in the drought and irrigation plots.

Because we did not monitor soil moisture directly in all X control, drought and irrigation plots, we used a model to describe the average treatment effects on soil moisture during the course of the experiment. To do this we first averaged observed soil moisture data from the dataloggers installed in four of the plot groups by date and plot and then within each plot group we found the average deviation from ambient soil moisture by subtracting the average soil moisture in the drought and irrigation plots from the average soil moisture in the nearby control areas. This left

us with a list of average daily deviations from ambient soil moisture in the drought and irrigation plots.

We expected that the effects the drought and irrigation experiment would have on soil moisture would depend on the season and whether it had rained recently. So we classified the daily climate during the experimental period into four seasons and classified each day as dry or rainy. Rainy days were defined as any days when average temperatures were above 3 degrees C and precipitation was over x mm. The day immediately following rainfall was also classified as rainy.

We modeled the average daily deviations in soil moisture and temperature in the treatments as a function of season, whether it had rained recently and the interaction between these two factors. After all this, we could then use this model to adjust the ambient soil moisture values predicted from the SOILWAT model above. These adjusted soil moisture values reflected the average season and rainfall dependent effects of the experimental treatments on soil moisture and could be used as covariates for predicting the effects of our manipulation on each species demographic rates.

Statistical models of vital rates

For each of the vital rates and each species we fit three separate models. First we fit a treatment model fit to all observations in the historical data as well as the contemporary experiment. This model included parameters estimating the effects of the drought and irrigation treatments on each species vital rate. This model was used to describe the basic results of the experiment. Next we fit two models to the historical observational data only (including the first four years of the modern data 2007 to 2010). We used these two models to generate predictions for the effects of the experiment. In the first prediction model, year to year variation in vital rates was treated as random effect. In the second prediction model, the "climate" model, we included paramaters that described the effects of year to year variation in seasonal soil moisture. These three models allow for two meaningful comparisons. First we can compare the predictions made by the two prediction models directly to the raw data in the experimental plots. In addition, we can compare the direction and magnitude of the soil moisture parameters estimated from the observational data by the climate model to the coefficients describing the treatment effects in the treatment model.

All three versions of the models of the models above follow the same basic structure and are developed from previous work (Adler et al., 2010; Chu and Adler, 2015). We model the survival

9

probability of an individual genet as a function of genet size, the neighborhood-scale crowding experienced by the genet from both conspecific and heterospecific genets, temporal variation among years, and permanent spatial variation among groups of quadrats ('group'; here means a set of nearby quadrats located within one pasture or grazing exclosure). In this analysis we only include crowding from the four main focal species.

Formally, we modeled the survival probability, S, of genet i in species j, group g, and removal treatmnt h, from time t to $t+1$ as

$$\text{logit}(S_{ijgh,t}) = \varphi_{jg}^{S} + \gamma_{j,t}^{S} + \beta_{j,t}^{S} u_{ij,t} + \left\langle \boldsymbol{\omega}_{j,t}^{S}, \boldsymbol{W}_{ij,t} \right\rangle \tag{1}$$

where φ is the spatial group dependent intercept, γ is a year-effect, β is year-dependent coefficient that represents the effect of log genet size, u, on survival in year t. $\boldsymbol{\omega}$ is a vector of interaction coefficients which determine the impact of crowding, $\boldsymbol{W}$, by each species on the focal species. The vector $\boldsymbol{W}$ includes crowding from the four dominant species, *A. tripartita*, *P. spicata*, *H. comata*, and *Poa secunda*. $\langle \boldsymbol{x}, \boldsymbol{y} \rangle$ denotes the inner product of vectors $\boldsymbol{x}$ and $\boldsymbol{y}$, calculated as `sum(x*y)` in R.

To describe the treatment effects in the experiment a new term is added to the above model,

$$\boldsymbol{T}\chi_{j}^{S} \tag{2}$$

where χ is a vector of treatment effect coefficients describing the effects of each experimental treatment h on the survival rate, and $\boldsymbol{T}$ is a design matrix indicating the treatment level of each observation in the data. The design matrix also includes terms for the interaction between plant size u and the treatment effects. These interaction terms allow the effect of each treatment to vary with plant size.

In the climate model, the χ and ξ terms are replaced with,

$$\boldsymbol{C}\xi_{j}^{S} \tag{3}$$

where ξ gives a vector of coefficients describing the effects of a set of soil moisture covariates $\boldsymbol{C}$ in treatment h and year t on the survival rate of species j. $\boldsymbol{C}$ is a vector of seasonal average soil

moisture and can include interaction effects between plant size, u, and the soil moisture covariates that allow the effects of soil moisture to vary with plant size.

Our growth model has a similar structure. The change in genet size from time t to $t+1$, conditional on survival, is given by:

$$u_{ijgh,t+1} = \varphi_{jg}^G + \gamma_{j,t}^G + \chi_{jh}^G + \beta_{j,t}^G u_{ij,t} + \left\langle \boldsymbol{\omega}_{j,t}^G, \boldsymbol{W}_{ij,t} \right\rangle + \varepsilon_{ij,t}^G. \tag{4}$$

To capture non-constant error variance in growth, we modeled the variance ε about the growth curve (4) as a nonlinear function of predicted genet size:

$$Var(\varepsilon_{ij,t}^G) = a \exp^{(b u_{ij,t+1})}. \tag{5}$$

As in the survival regression above, specific specific parameters describing the treatment effects on growth are added in the treatment model,

$$\boldsymbol{T} \chi_j^G \tag{6}$$

where χ is a treatment effect describing the effect of experimental treatment h on growth, including treatment by size interactions.

Similarly, in the climate model soil moisture influences the growth equation through these terms,

$$\boldsymbol{C} \xi_j^G \tag{7}$$

where ξ is a vector of coefficients describing the effects of soil moisture covariates in the matrix $\boldsymbol{C}$ for treatment h and year t on growth of species j. Again this can include interactions between soil moisture and plant size u.

Although the main focus of the current analysis the effects of soil moisture, we also modeled the effects of inter- and intra-specific competition in our vital rate models. We model the crowding experienced by a focal genet as a function of the distance to and size of neighbor genets. In previous work, we assumed that the decay of crowding with neighbor distance followed a Gaussian function (Chu and Adler, 2015), but here we use a data-driven approach (Teller et al., 2016; **?**). We model

the crowding experienced by genet i of species j from neighbors of species m as the sum of neighbor areas across a set of concentric annuli, k, centered at the plant,

$$w_{ijm,k} = F_{jm}(d_k)A_{i,k} \tag{8}$$

where F_{jm} is the competition kernel (described below) for effects of species m on species j, d_k is the average of the inner and outer radii of annulus k, and $A_{im,k}$ is the total area of genets of species m in annulus k around genet i. The total crowding on genet i exerted by species m is

$$W_{ijm} = \sum_k w_{ijm,k}. \tag{9}$$

Note that W_{ijj} gives intraspecific crowding. The W's are then the components of the $\boldsymbol{W}$ vectors introduced as covariates in the survival (1) and growth (4) regressions.

We assume that competition kernels $F_{jm}(d)$ are non-negative and decreasing, so that distant plants have less effect than close plants. Otherwise, we let the data dictate the shape of the kernel by fitting a spline model using the methods of Teller et al. (2016). The shape of F_{jm} is determined by a set of spline basis coefficients $\vec{b}_{jm}$ and a smoothing parameter η that controls the complexity of the fitted kernel. Demographic models such as (1) then have γ, φ, χ, β, $\boldsymbol{\omega}$, $\vec{b}$ and η as parameters to be fitted. We implemented this in the statistical computing environment, R, by making the spline coefficients and η the arguments of an objective function that computes $\boldsymbol{W}$ using the input spline coefficients, calls the model-fitting functions `lmer` and/or `glmer` to fit the other parameters in the survival and growth regressions, and returns an approximate AIC value and model degrees of freedom (df) for survival and growth combined. We used the $\vec{b}$ values at the smoothest local minimum of AIC as a function of df, as in Teller et al. (2016). This approach assumes that one measure of crowding affects survival and growth. In addition, for fitting the kernels we assumed that survival and growth depended only on intraspecific crowding, and thus only fitted the within-species competition kernels F_{jj}. Based on previous work (Adler et al., 2010), we set all F_{mj} equal to F_{jj}, meaning that the within-species competition kernel for species j is also used to determine the effect of all other species on species j. We used data from all historical plots and contemporary control-treatment plots to estimate the competition kernels (**?**).

12

Once we had estimated the competitions kernels, we used them to calculate the values of $\boldsymbol{W}$ for each individual, and fit the full survival and growth regressions, which include the interspecific interaction coefficients, $\boldsymbol{\omega}$. All genets in a quadrat were included in calculating W, but plants located within 5 cm of quadrat edges were not used in fitting.

We model recruitment at the quadrat level rather than at the individual genet level because the mapped data do not allow us to determine which recruits were produced by which potential parent plants. We assume that the number of individuals, y, of species j recruiting at time $t+1$ in the location q follows a negative binomial distribution:

$$y_{jq,t+1} = NegBin(\lambda_{jq,t+1}, \theta) \tag{10}$$

where λ is the mean intensity and θ is the size parameter. In turn, λ depends on the composition of the quadrat in the previous year:

$$\lambda_{jq,t+1} = C'_{jq,t} \exp\left(\varphi^R_{jg} + \gamma^R_{j,t} + \left\langle \boldsymbol{\omega}^R, \sqrt{\boldsymbol{C'}_{\boldsymbol{q,t}}} \right\rangle\right) \tag{11}$$

where the superscript R refers to Recruitment, $C'_{jq,t}$ is the 'effective cover' (cm^2) of species j in quadrat q at time t, φ is a group dependent intercept, γ is a random year effect, $\boldsymbol{\omega}$ is a vector of coefficients that determine the strength of intra- and interspecific density-dependence, and $\boldsymbol{C'}$ is the vector of "effective" cover of each species in the community. Following previous work (Adler et al., 2010), we treated year as a random factor allowing intercepts to vary among years.

Because plants outside the mapped quadrat could contribute recruits to the focal quadrat or interact with plants in the focal quadrat, we estimated effective cover as a mixture of the observed cover, C, in the focal quadrat, q, and the mean cover, $\bar{C}$, across the spatial location, g, in which the quadrat is located: $C'_{jq,t} = p_j C_{jq,t} + (1 - p_j)\bar{C}_{jg,t}$, where p is a mixing fraction between 0 and 1 that was estimated as part of fitting the model.

In the treatment model, a new term is added to the exponential term in the equation above,

$$\boldsymbol{Tchi}^R_j \tag{12}$$

where chi describes the effect of the treatment levels on recruitment.

₃₁₆ Likewise in the climate model this term is added,

$$\boldsymbol{C}\xi_j^R \tag{13}$$

₃₁₇ where the $\boldsymbol{\xi}$ gives a set of coefficients for the soil year, and treatment specific soil moisture covariates
₃₁₈ in $\boldsymbol{C}$.

₃₁₉ We fit all vital rate models using Hamiltonian-Markov Chain Monte Carlo (HMCMC)
₃₂₀ simulations in STAN 6.4 (**?**) and (**?**). The priors and model code are described more completely
₃₂₁ in appendix A. Each model was run for 2,000 iterations and four independent chains with different
₃₂₂ initial values for parameters. We discarded the initial 1,000 samples. Convergence was observed
₃₂₃ graphically for all parameters, and confirmed by assessing the split $\widehat{R}$ statistic which at convergence
₃₂₄ is equal to one (**?**).

₃₂₅ To assess the effects of the experimental treatments on species survival and growth we fit
₃₂₆ treatment models with and without the size by treatment interactions in the treatment effect term
₃₂₇ for (2) and growth models (6). We judged whether including interaction terms improved model fit by
₃₂₈ comparing the Watanabe-Aikake Information Criteria (WAIC) scores for each version of the model
₃₂₉ and retained the version with the lower WAIC score (**?**). WAIC scores approximate cross-validation
₃₃₀ predictive accuracy for a model and like traditional AIC allow for model comparison. Lower WAIC
₃₃₁ scores indicate a more parsimonious model. When a treatment model for survival or growth for
₃₃₂ a species included a size by treatment effect, we also included a size by soil moisture effect in the
₃₃₃ climate model for that species and vital rate. This allowed us to more directly compare the effects
₃₃₄ in the experimental data to the effects predicted from the climate model fit to the observational
₃₃₅ data.

₃₃₆ Selecting soil moisture covariates

₃₃₇ After generating a time series of predicted daily soil moisture from the SOILWAT model, we
₃₃₈ averaged daily soil moisture across spring, summer and fall seasons in each year. We considered
₃₃₉ each of the three seasonal soil moisture variables at three different time periods relative to the
₃₄₀ demographic transition from year t to year $t + 1$. Soil moisture in the year between t and $t + 1$ is
₃₄₁ indicated with a "1" subscript. Soil moisture in the year before t is indicated with a "0" subscript.

14

And soil moisture preceding this year is indicated with a "lag" subscript. For example, for the year 2010, $spring_1$ would indicate soil moisture in the spring of 2010, $spring_0$ would indicate soil moisture during the spring of 2009 and $spring_{lag}$ would indicate soil moisture during the spring of 2008.

In order to select among the nine potential soil moisture covariates (three seasons and three lags each) for each species and vital rate, we first fit a model with random year effects but without climate covariates to the observational data up to 2010. We then extracted the mean of the year effects estimates for each fitted year in the data. These random effects represented unexplained deviations in the average vital rate in a given year. We then found the correlations between each of the soil moisture variable and the random year effects. For each vital rate and species, we selected the three covariates with highest correlations with these year effects. This screening technique has been used in previous demographic studies at this site (**?**) and is often used in dendrochronology to screen for potential climate influence on tree-ring growth (**?**); however, it is subject to the criticism that it is a form of data dredging (**?**). Nevertheless, we felt that this approach was justified in this study because ultimately we did not make inference from these fitted parameters until after we tested their ability to predict the data in the experimental plots.

Once we selected soil moisture covariates for each of the species and vital rates we fit the climate models including the climate terms for survival 3, growth 7 and recruitment 13. We fit these models only to the observational data from the historical period and (1928 to 1957) and the first four years of the modern period (2007 to 2010). Thus in generating predictions for the treatment effects observed in from 2011 to 2016 we are predicting truly out of sample data.

Predicting cover from individual-based models

The vital rate regressions allow us to evaluate whether soil moisture and the experimental treatments had an effect on species performance. But the population response ultimately depends on the integrated effects of treatment or soil moisture on all three vital rates. To evaluate whether the climate models could predict the responses of these species in the drought and irrigation experiment at the overall population level we used an individual-based model (IBM) to compare observed and predicted changes in population size from one year to the next.

370   To simulate changes in cover in each quadrat from year t to year $t + 1$, we initialized the

371   IBM with the observed genet sizes and locations of the four focal species observed in year t in each

372   quadrat. For every individual genet in a quadrat, we projected its size and survival probability in

373   the next year using the growth and survival models and the appropriate crowding and soil moisture

374   or treatment covariates for that year and quadrat. Likewise we projected the number of new recruits

375   in the quadrat in the next year using the recruitment model. We calculated the expected cover in

376   year $t+1$ as the total area of new recruits, plus the sum of the predicted area of each existing plant

377   at time $t + 1$ multiplied by each plant's expected survival probability from time t to $t + 1$.

378   We accounted for the uncertainty in our random year effects when generating predictions,

379   by drawing random year effects for each predicted year from a normal distribution with a mean

380   of zero and a standard deviation drawn from the posterior estimate of the standard deviation of

381   the random year effects **??**. We generated predictions using the full posterior distributions of each

382   model parameter which allowed us to carry forward all of the uncertainty of the fitted vital rate

383   models into our cover predictions. Because we were interested in comparing model predictions

384   to observations, and were not interested in the effects of demographic stochasticity, we used a

385   deterministic version of the models (e.g., recruitment is the λ of (11), rather than a random draw

386   from a negative binomial distribution with a mean of λ).

387   We generated predictions for the full time series of observations, including the five exper-

388   imental years, from the year effects model, the climate model and the treatment model. After

389   generating predictions for each year, we found the mean cover across all quadrats in each treatment

390   level and then calculated the predicted log cover change as $log(Cover_{t+1}/Cover_t)$.

Quantifying predictive accuracy

392   After fitting the year effects and climate models to the observational data, we generated predic-

393   tions from these models for each of the vital rates in the experimental plots. We then assessed

394   performance of the climate and null models by calculating the mean square error (MSE) between

395   the predicted and observed responses in the experimental data as,

$$MSE = \frac{1}{n} \sum_{i=1}^{n} (y_i - E(y_i|\theta))^2, \tag{14}$$

where y_i is the outcome of observation i and $E(y_i|\theta)$ gives the expected outcome given the parameters in the model θ. The MSE is easy to interpret, but is not always appropriate for models fit with non-normal error structures (**?**). A more general statistic for assessing model predictions is the log pointwise predictive density (lppd) (**?**). The lppd for a given model is defined as,

$$lppd = \sum_{i=1}^{n} log \int p(y_i|\theta)p_{post}(\theta)d\theta, \tag{15}$$

where the integral on the right side gives the probability of observing the outcome y at each data point i given the full posterior distribution of the parameters in the model $p_{post}(\theta)$. In practice we computed the lppd from the posterior simulations generated by STAN as,

$$\widehat{lppd} = \sum_{i=1}^{n} log \left(\frac{1}{S} \sum_{s=1}^{S} p(y_i|\theta^S) \right), \tag{16}$$

where the summation of $p(y_i|\theta^S)$ gives the total probability of observing the the actual response y_i given the simulated posterior distribution θ^S across the full set of model simulations S. The log of this sum is then averaged across the set of all observations i. Higher lppd scores indicate that the model better predicts the observations.

In addition, we evaluated whether the climate model predicted treatment effects of similar direction and magnitude to those observed in the experiment. We did this by extracting the soil moisture coefficients contained in ξ for each of the vital rates and then multiplying those by the appropriate soil moisture covariates for each year and treatment level in the experiment. We then averaged these across all five years in the experiment to find the average treatment effect predicted by the climate model. We compared these to the posteriors of the treatment parameters, chi, from the treatment model. As a measure of agreement between our predictions and observed response we calculated the correlation between the predicted and observed parameter values.

We considered the effect of climate covariates or treatment effects to be significant when the 95% Bayesian credible intervals on the posterior estimates did not overlap zero.

All data and R code necessary to reproduce our analysis will be deposited in the Dryad Digital Repository once the manuscript is accepted. The current version of the computer code

17

is available at https://github.com/pbadler/ExperimentTests/tree/master/precip and the data are available at https://bitbucket.org/ellner/driversdata.

Results

Effects on soil moisture

Our treatments succussfully changed the soil moisture in our experimental plots in the directions expected (fig): our hand held spot measurements of soil moisture conducted during the springs of 2012, 2015 and 2016 showed that drought plots were X percent drier, while irrigation plots were X percent wetter than ambient plots. This difference was highly significant.

The automatically recorded soil moisture data from only half of the experimental plots also showed that the drought treatment decreased and the irrigation treatment increased soil moisture, but the size of these effects were dependent on season and whether it had rained recently (). The best model for predicting the average treatment effects on soil moisture was : . We did not find evidence that the drought shelters and the irrigation treatments significantly changed air temperature within the plots ().

The SOILWAT soil moisture model indicated that soil moisture fluctated from between X and X on average each year, with the months of X and X being the wettest while soil moisture during the months of X and X was driest (fig). Predicted seasonal soil moisture for each year was positively correlated with precipitation, and negatively correlated with average temperatures. The average soil moisture predicted from soilwat for the entire study period from X to X is shown in figure X. Soil moisture predictions for the ambient conditions from 2011 to 2016 fall on the low side of the period of record averages. This was driven by higher than average temperatures and severely dry winters and spring conditions in the years of X.

When we adjust the seasonally averaged soil moisture predictions by the treatment effects, we find that the soil moisture conditions predicted in the drought plots during the course of the experiment are lower than those predicted for any of the previous years in the historical record. Likewise the predicted soil moisture in the irrigation plots was far above the average for the historical record in the years of X and X. We interpret this as evidence that our drought and irrigation plots created truly novel soil moisture conditions in the years X and X that were unlikely to have ever been

18

experienced by the study species during the entire period of the observational data. We visualize this by conducting a principle component analysis (PCA) on all the seasonal soil moisture, and plotting each year on the first two principle components. The PCA shows that the ambient, drought and irrigation plots experienced warmer than average seasonal conditions during the course of the experiment (further left on PCA1). The drought plots were considerably drier, and the irrigated plots considerably wetter (figure PCA).

Effects on cover and vital rates

The cover of *H. comata* and *P. spicata* fell significantly by X and X percent respectively from the pre-treatment cover in 2011 to 2016. The cover of *P. secunda* showed a trend towards decrease in the drought plots and an increase in the irrigated plots but these changes were not significant. In contrast the cover of *A. tripartita* changed in the opposite direction from the grasses; it increased in the drought plots and decreased in the irrigated plots but these changes were not significant (fig).

Our treatment models fit to the experimental and observational data indicated a variety of treatment effects on the vital rates of each species (table x). Among the survival models, WAIC scores indicated that we should retain size x treatment effects for *P. secunda*. Among the growth models, we retained size by treatment effects for *A. tripartita* and *P. secunda*. DISCUSS SIGNIFICANT treatment effects: For *A. tripartita* we observed a significant decrease in growth in the x treatment, while we observed no change in the X treatment. *H. comata* growth, survival and recruitment, while growth. *P. secunda* growth and survival recruitment. *P. spicata* growth survival and recruitment. Treatment by size effects on *A. tripartita* and *P. secunda* showed that ()

We observed a number of strong correlations between the year effects in the vital rate models and the seasonal soil moisture variables and table x reports the strongest three correlations for each species and vital rate (table). In general the soil moisture during the spring and summer period appeared to be more strongly correlated with the year effects for each species than the fall soil moisture, but see *P. spicata* vr. All three time lags show up in the choosen variables, but 1 out of X variables choosen involved soil moisture in the year immediately before the first year of the transition, (subscript "0"), while variables involving soil moisture in the year before that (subscript "lag") and after that (subscript "1") were choosen less often.

19

We observed vital rate and species-specific effects of soil moisture on each of these species after fitting the vital rate models with the soil moisture covariates discussed above (fig). DISSCUSS significant soil moisture effects: for *A. tripartita* growth was significantly affected by ... For *H. comata*. For *P. secunda*. And for *P. spicata*. Soil moisture by size effects on *A. tripartita* and *P. secunda* showed that ()

Evaluating the predictions

For each vital rate and species, predictions from the year effects and climate models were nearly indistinguishable (fig). This indicated that the additional soil moisture covariates in the climate models had very little effect on the predictions. Not surprisingly (**??**) our models show that plant size and intra-specific crowding are far more influential in determining growth, survival and recruitment than climate effects. In all cases, we found MSE and lppd scores for the climate models were slightly worse than the MSE and the lppd of the year effects model (table). This indicated that adding the soil moisture parameters did not improve model predictions over all (table). When we break the data up into treatment groups we do see that the climate model outperformed the year effects model for predicting X species VR in treatment T.

While our climate models failed to improve predictions, we did find that they predicted treatment responses that were largely in the same direction as the observed treatment responses (fig). The overall correlation between the predicted treatment parameters and the observed treatment parameters was X with stronger correlation for the climate effects on the size by treatment effects fit for *P. secunda* growth and survival and *A. tripartita* growth (fig) than for the treatment effects on the intercept. A table of MSE between predicted and expected treatment parameters shows that averaged over all species and vital rates, we did the best job of predicting the response to the drought treatment. Averaged across all treatements and vital rates, we did the best job predicting the response of *species* to the treatments. Finally if we average across all species and treatments, we did the best job of predicting VR parameters in response to the treatment.

As for the vital rate predictions, our one-step ahead cover predictions from the year effects models and the climate models were fairly similar (fig). Models with and without soil moisture parameters tended to underpredict the cover of *A. tripartita* and *P.secunda* during the experiment (fig). When we compare the MSE of the predicted population growth rates for each year and

20

quadrat from the model with and without the soil moisture parameters, we find that adding soil moisture to the vital rate models always made the one step ahead cover predictions slightly less accurate (table). The pattern when we consider the correlation between the predicted and observed population growth rates was slightly different (table?). When we considered the population growth rate data separately by treatment, we found that adding soil moisture to the models mostly did not improve predictions of cover change in the control and irrigation plots. However, we did find that adding soil moisture parameters produced better predictions of population growth rates for three of the species (S , S, and S) in the drought plots (fig).

As expected from previous research most of our demographic models estimated strong negative intra-specific crowding effects and weaker negative inter-specific crowding effects on the focal species (appendix) (Adler et al., 2010; ?; Chu and Adler, 2015).

(Fig. 2), but shrub removal did appear to cause an increase in the cover of *P. spicata*. We tested the effects of removal on cover by analyzing year-to-year changes in (log) cover, a measure of population growth rate (Fig. 3). The removal treatments had no significant effect on *A. tripartita* (95% confidence interval on removal treatment effect: -0.75, 0.56) or *Poa secunda* (95% CI: -0.41, 0.25) population growth, but did increase *H. comata* (95% CI: 0.01, 0.65) and *P. spicata* (95% CI: 0.01, 0.40) population growth (Table SI-1). However, these treatment comparisons do not address our questions about whether responses to removal were adequately predicted by models fit to observational data on non-removal plots.

Vital rates

Our vital rate models take into account the effects of local species composition and should therefore be able to predict the effect of removals on survival, growth and recruitment without any additional parameters. If the removal treatment effects that we added to these models are statistically significant, it would indicate an effect of removals that goes above and beyond the response predicted by a model based on data from the control plots. For the survival models, the 95% confidence intervals on the removal effects overlapped zero for all four species (Fig. **??**; Tables SI-2 to SI-5), meaning that the survival probabilities of plants in removal plots can be predicted based on data from control plots. However, for the growth models, the 95% confidence intervals on the removal effects were positive for *Poa secunda* and *P. spicata*, meaning that individuals of these species grew

more rapidly in removal plots than controls even after accounting for neighborhood interactions (Fig. **??**; Tables SI-6 to SI-9). In contrast, *Poa secunda* had lower recruitment in removal than controls plots (upper limit of 95% CI < 0; Fig. **??**; Table SI-14).

The positive removal effects on *Poa secunda* and *P. spicata* growth are particularly interesting, because they suggest that models based on observational data may underestimate competitive release. We conducted additional analyses to further explore removal effects on the growth of these two species. First, we classified all individuals of these species as located either inside or outside the limits of *A. tripartita* canopies present in 2011 (before removal). If removal is releasing grasses from *A. tripartita* competition, we would expect individuals located under the shrub canopies to experience a greater effect of removal. However, the location of individuals with respect to *A. tripartita* canopies had no effect on growth of either species (Tables SI-10 and SI-11), meaning that individuals located outside *A. tripartita* canopies responded to removals as much as individuals underneath (removed) canopies.

Second, we evaluated the possibility that removal effects might be transient. We removed aboveground plant material, but roots of the removed plants remain in the ground and decompose, potentially creating a flush of mineral nutrients. We tested for a transient removal effect by adding a year-by-treatment interaction. For both *Poa secunda* and *P. spicata* , we found no sign of a decrease in the removal effect over time (Tables SI-12 and SI-13).

Third, responses to removals might be poorly predicted by models based on observational data if the removals create local crowding outside the range of historical variation or if the removals break covariances in crowding among species. However, the distribution of crowding observed within control plots easily spans the crowding values observed in removal plots (Fig. **??**), and we failed to find evidence for strong interspecific covariances in crowding (Section SI.1).

Finally, we evaluated pre-existing differences in community composition in removal and control plots. In selecting removal plots, our criteria required candidate plots to include a certain amount of our target removal species. Because we adopted the historical plots as our controls, the same criteria were not applied (a control plot might not contain any *A. tripartita*). To quantify resulting differences in pre-treatment (2011) composition, we compared neighborhood crowding at the individual plant level (the W of the growth regression) across treatments. *A. tripartita* crowding and crowding by all subdominant shrub and grass species appeared greater than in the controls,

22

whereas crowding by *H. comata* was lower in removal plots than controls, though it was absent from most *P. spicata* neighborhood in both treatments (Fig. **??**). These pre-existing differences in composition raise the possibility that plots selected for the removal treatments might differ from the control plots in some unobserved covariate that could influence plant performance.

Population-level responses

To quantify the short-term population-level consequences of removals, we used an IBM to project the cover of each species in each quadrat one year ahead using versions of the model with and without removal treatment effects. Our models tended to under-predict population growth (Fig. 3) and population size (Fig. **??**) for all species, but the difference between predictions from the baseline and removal models varied among species. For *A. tripartita*, both observed and predicted population growth rates were close to zero, and differences in model predictions were small. *H. comata* experienced greater variation in growth rates, but the inclusion of removal treatment effects had little effect on population growth rates. For *Poa secunda* and especially *P. spicata*, the model with removal effects consistently predicted higher population growth than the baseline model (Fig. 3), and reduced the underestimates of cover (Fig. **??**). The version of the model with maximum removal treatment effects (removal coefficients set to the 95% confidence limit furthest from zero), were qualitatively similar, but further amplified the contrast between predictions of the baseline and removal models for and *P. spicata* (Fig. **??**).

To quantify the long-term population-level consequences of removals, we used an IPM to project stochastic equilibrium cover. We concentrated on grass species' responses to *A. tripartita* removal, since the growth regressions indicated our baseline model might underestimate competitive release in this situation (our baseline vital rate models worked well in predicting *A. tripartita* responses to grass removal). Using the baseline model, with no removal treatment coeffiicients, the IPM predicts little effect of *A. tripartita* removal on the cover of any grass species (compare gray and brown boxes in Fig. **??**). Using a model with removal treatment coefficients, the IPM predicts little effect of shrub removal on *Poa secunda* and *H. comata*, but a 2-fold increase in the cover of *P. spicata* (Fig. **??**). Running a version of the model with maximum removal treatment effects (removal coefficients set to the 95% confidence limit furthest from zero), resulted in the same qualitative outcome, but a larger increase in *P. spicata* (Fig. **??**).

The equilibrium cover of Artemisia simulated by the IPM (6.0%) is consistent with observed cover during the historical data collection period (6.6% from 1931-1956), but is low compared to contemporary observed cover (15-25%,2). Could the small competitive release following simulated Artemisia removal simply reflect the low Artemisia cover? To explore this possibility, we increased Artemisia cover in the baseline simulation by increasing average Artemisia fecundity. The increased fecundity led to a doubling of Artemisia average cover, but had essentially zero effect on the cover of the grasses (changes of less than 0.1% cover).

Discussion

Our experiment showed that including climate covariates in our population models did little to improve population level predictions across the course of the experiment. Averaged across the control, drought and irrigation treatments, the climate models did not perform as well as null models in predicting response the experiment at the vital rate or at the level of population growth rates. However, there were some glimmers of hope. First at the population level we generally found that including climate covariates did not improve predictions in the control and irrigation plots, but they did appear to improve predictions in the drought plots (). This suggests that models fit to observational data do contain useful information about the effects of climate on individual performance. The fact that these predictions showed up in the more extreme conditions produced by the drought plots could be a sign that in ambient conditions the effect of climate is weak enough that it is washed out at the population level by finer scale sources of variation. This pattern was observed for species x, x and x.

the climate signal improve population growth predictions in the drought treatment but not experiment showed some relatively strong reson based on historical, observational data reveal weak interspecific interactions (Adler et al., 2010; Chu and Adler, 2015) and, as a result, predict very little competitive release among the four dominant species in a sagebrush steppe. Despite the fact that previous removal studies have reported variable results, ranging from negative effects of removal on remaining species to complete competitive release, we were suspicious of our model's predictions and conducted a removal experiment to test them. The results provide substantial support for our model's predictions.

24

For three of the four species, we find little or no evidence that models based on observational data underestimate the intensity of interspecific competition. Removal treatment effects were never significant for *A. tripartita* or *H. comata*; our baseline model, which accounts for local neighborhood composition, adequately explained vital rate responses to removal. *Poa secunda* showed mixed responses to *Artemisia* removal: removal effects were not significant at the survival stage, were positive at the growth stage, and negative at the recruitment stage (where the estimated effect of *Artemisia* on *Poa* is positive). At the population level, models with and without removal effects projected similar patterns of short (Fig. **??**) and long-term (Fig. **??**) dynamics for *H. comata* and *A. tripartita*. For *Poa secunda*, the model with removal effects predicted higher population growth over the short but not the long-term, perhaps because the short-term projections mostly reflect the positive effect of *Artemisia* removal on growth, while the long-term equilibrium are also sensitive to the negative effects of removal on recruitment. Although the baseline model did not always successfully predict removal effects on vital rates, it does appear to successfully capture the population-level consequences of removals on these three species and did not severely underestimate the magnitude of competitive release.

The story is different for the fourth species, *P. spicata*. Both individual growth and short- and long-term population growth were higher in the sagebrush removal treatments than in the control plots, suggesting that our analyses of observational data may underestimate the competitive release that *P. spicata* experiences following *Artemisia* removal. However, the mechanism by which *Artemisia* removal promotes *P. spicata* remains unclear. If *Artemisia* removal is releasing *P. spicata* from competition, we should expect *P. spicata* individuals that were located beneath *Artemisia* shrubs that we removed to respond more than individuals located away from any shrubs. Yet we found no evidence for such a difference. An alternative explanation involves pre-treatment differences in composition between control plots and the *Artemisia* removal plots, which had higher cover of *Artemisia* (see 2011 means in Fig. 2) and higher cover of subdominant grasses and shrubs (Fig. **??**). Perhaps these pre-treatment differences reflect subtle differences in edaphic and environmental factors which could promote *P. spicata* growth. While *P. spicata* appears to show stronger competitive release than our baseline model predicted, the evidence is not conclusive.

The small competitive release of many species in our system implies that each of the four dominant species we studied are limited by quite different factors. This low niche overlap could

reflect strong resource partitioning (Tilman 1982), perhaps combined with variation in the times and locations at which species are taking up those resources. Species-specific responses to spatial and temporal variation in non-resource environmental variables can also weaken interspecific interactions (Chesson, 2000), though in a previous study we failed to find evidence of a temporal storage effect in this community (Adler et al., 2009). Interactions with above- or belowground enemies can regulate populations and, given enough species-specificity in the effects of these enemies, decouple interspecific dynamics (Hersh et al., 2011; Janzen, 1970; Connell, 1971). More likely, plants may alter the environment, and even resource availability, in ways that facilitate their neighbors. For example, shade cast by *Artemisia* canopies may reduce evapotranspiration (e.g. Barbier 2008). *Artemisia* removal might offest this facilitative effect by reducing resource uptake, resulting in little net change in water balance following removal. Unfortunately, we did not monitor soil moisture at the fine spatial and temporal resolution necessary to test this hypothesis.

Evidence for weak interspecific interactions and limited competitive release carries interesting implications. If most interspecific interactions are weak, then single-species models may be adequate for forecasting population responses to environmental change (Adler et al., 2012; Kleinhesselink and Adler, 2015). Similarly, differences among species in relative abundance should reflect variation in the strength of intraspecific density dependence more than variation in the strength of interspecific interactions (Yenni et al., 2012). In such a system, effective management and conservation requires understanding the sources and species-specificity of intraspecific density dependence. In fact, an experiment to test our model's skill at predicting release from intraspecific competition could be more important than the test of interspecific competitive release described here.

Our results have given us more confidence that competitive release is quite small for the dominant species in our study system. But for many species in other communities, interspecific competition may still be an important driver. In closed-canopy forests where competition for light is intense, we might have found different results than in our system, in which competition for a number of belowground resources is more important than competition for light. However, a number of recent studies from forests have also found that heterospecific competitive effects are dramatically weaker than conspecific effects (Comita et al., 2010; Kunstler et al., 2015; Johnson et al., 2012). We also expect stronger competitive release in successional systems, or communities in the early stages of community assembly where the process of competitive exclusion is still underway

26

(Kokkoris et al., 1999). Finally, we might have found stronger competitive release if we could have studied rare species in our system, as long as those species are rare because of niche overlap with stronger competitors. If they are rare because they occupy unique, but narrow, niches, interspecific interactions would still be weak. Determining why interspecific interactions and competitive release are strong in some ecological contexts but weak in others remains a fascinating research problem.

Acknowledgements

References

Aarssen, L. W. and G. A. Epp. 1990. Neighbour manipulations in natural vegetation a review. Journal of Vegetation Science, **1**:13–30.

Adler, P. B., H. J. Dalgleish, and S. P. Ellner. 2012. Forecasting plant community impacts of climate variability and change: when do competitive interactions matter? Journal of Ecology, **100**:478–487.

Adler, P. B., S. P. Ellner, and J. M. Levine. 2010. Coexistence of perennial plants: an embarrassment of niches. Ecology Letters, **13**:1019–1029.

Adler, P. B., J. HilleRisLambers, and J. M. Levine. 2009. Weak effect of climate variability on coexistence in a sagebrush steppe community. Ecology, **90**:3303–3312.

Barbier, N. C. 2008. Spatial decoupling of facilitation and competition at the origin of gapped vegetation patterns. ECOLOGY, **89**:1521–1531.

Bates, D., M. Mächler, B. Bolker, and S. Walker. 2015. Fitting linear mixed-effects models using lme4. Journal of Statistical Software, **67**:1–48.

Belsky, A. J. 1992. Effects of grazing, competition, disturbance and fire on species composition and diversity in grassland communities. Journal of Vegetation Science, **3**:187–200.

Brooker, R. W., F. T. Maestre, R. M. Callaway, C. L. Lortie, L. A. Cavieres, G. Kunstler, P. Liancourt, K. TielbRger, J. M. J. Travis, F. Anthelme, C. Armas, L. Coll, E. Corcket, S. Delzon, E. Forey, Z. Kikvidze, J. Olofsson, F. Pugnaire, C. L. Quiroz, P. Saccone, K. Schiffers, M. Seifan, B. Touzard, and R. Michalet. 2008. Facilitation in plant communities: the past, the present, and the future. Journal of Ecology, **96**:18–34.

Brooks, S. and A. Gelman. 1998. General methods for monitoring convergence of iterative simulations. Journal of Computational and Graphical Statistics, **7**:434–455.

Chesson, P. 2000. Mechanisms of maintenance of species diversity. Annual Review of Ecology & Systematics, **31**:343–366.

715 Chu, C. and P. B. Adler. 2015. Large niche differences emerge at the recruitment stage to stabilize
716   grassland coexistence. Ecological Monographs, **85**:373–392.

717 Comita, L. S., H. C. Muller-Landau, S. Aguilar, and S. P. Hubbell. 2010. Asymmetric density
718   dependence shapes species abundances in a tropical tree community. Science, **329**:330–332.

719 Connell, J. 1971. On the role of natural enemies in preventing competitive exclusion in some marine
720   animals and in rain forest trees. In P. J. Den Boer and G. R. Gradwell, editors, Dynamics of
721   Populations, pages 298–312. PUDOC, Wageningen.

722 Ellner, S. P., D. Z. Childs, and M. Rees. 2016. Data-driven Modelling of Structured Populations.
723   Lecture Notes on Mathematical Modelling in the Life Sciences, Springer International Publishing,
724   Cham.

725 Gilbert, B., R. Turkington, D. Srivastava, A. E. O. J. Schmitz, and E. D. L. DeAngelis. 2009.
726   Dominant species and diversity: linking relative abundance to controls of species establishment.
727   The American Naturalist, **174**:850–862.

728 Grime, J. P. 1979. Plant strategies and vegetation processes. John Wiley & Sons, New York.

729 He, Q., M. D. Bertness, and A. H. Altieri. 2013. Global shifts towards positive species interactions
730   with increasing environmental stress. Ecology Letters, **16**:695–706.

731 Hersh, M. H., R. Vilgalys, and J. S. Clark. 2011. Evaluating the impacts of multiple generalist
732   fungal pathogens on temperate tree seedling survival. Ecology, **93**:511–520.

733 Hubbell, S. P. 2001. The unified neutral theory of biodiversity and biogeography. Princeton
734   University Press, Princeton, N.J.

735 Janzen, D. H. 1970. Herbivores and the number of tree species in tropical forests. The American
736   Naturalist, **104**:501–528.

737 Johnson, D. J., W. T. Beaulieu, J. D. Bever, and K. Clay. 2012. Conspecific negative density
738   dependence and forest diversity. Science, **336**:904–907.

Jutila, H. M. and J. B. Grace. 2002. Effects of disturbance on germination and seedling estab-
lishment in a coastal prairie grassland: a test of the competitive release hypothesis. Journal of
Ecology, **90**:291–302.

Keddy, P. A. 1989. Effects of competition from shrubs on herbaceous wetland plants: a 4-year field
experiment. Canadian Journal of Botany, **67**:708–716.

Kleinhesselink, A. R. and P. B. Adler. 2015. Indirect effects of environmental change in resource
competition models. The American Naturalist, **186**:766–776.

Kokkoris, G., A. Troumbis, and J. Lawton. 1999. Patterns of species interaction strength in assem-
bled theoretical competition communities. Ecology Letters, **2**:70–74.

Kunstler, G., D. Falster, D. A. Coomes, F. Hui, R. M. Kooyman, D. C. Laughlin, L. Poorter,
M. Vanderwel, G. Vieilledent, S. J. Wright, M. Aiba, C. Baraloto, J. Caspersen, J. H. C. Cor-
nelissen, S. Gourlet-Fleury, M. Hanewinkel, B. Herault, J. Kattge, H. Kurokawa, Y. Onoda,
J. Peuelas, H. Poorter, M. Uriarte, S. Richardson, P. Ruiz-Benito, I.-F. Sun, G. Sthl, N. G.
Swenson, J. Thompson, B. Westerlund, C. Wirth, M. A. Zavala, H. Zeng, J. K. Zimmerman,
N. E. Zimmermann, and M. Westoby. 2015. Plant functional traits have globally consistent effects
on competition. Nature, **advance online publication**.

Lauenroth, W. K. and P. B. Adler. 2008. Demography of perennial grassland plants: survival, life
expectancy and life span. Journal of Ecology, **96**:1023–1032.

Leps, J. 1999. Nutrient status, disturbance and competition: an experimental test of relationships
in a wet meadow copy. Journal of Vegetation Science, **10**:219–230.

Lunn, D. J., A. Thomas, N. Best, and D. Spiegelhalter. 2000. WinBUGS - A Bayesian modelling
framework: Concepts, structure, and extensibility. Statistics and Computing, **10**:325–337.

Metcalf, C. J. E., S. P. Ellner, D. Z. Childs, R. Salguero-Gmez, C. Merow, S. M. McMahon,
E. Jongejans, and M. Rees. 2015. Statistical modelling of annual variation for inference on
stochastic population dynamics using Integral Projection Models. Methods in Ecology and Evo-
lution, **6**:1007–1017.

765 Ricker, W. E. 1954. Stock and recruitment. Journal of the Fisheries Research Board, **11**:559–623.

766 Rue, H., S. Martino, and N. Chopin. 2009. Approximate Bayesian inference for latent Gaussian
767   models by using integrated nested Laplace approximations. Journal of the Royal Statistical
768   Society: Series B (Statistical Methodology), **71**:319–392.

769 Sala, O. E., R. A. Golluscio, W. K. Lauenroth, and A. Soriano. 1989. Resource partitioning between
770   shrubs and grasses in the Patagonian steppe. Oecologia, **81**:501–505.

771 Silvertown, J. 2004. Plant coexistence and the niche. Trends in Ecology and Evolution, **19**:605–611.

772 Smith, M. D. and A. K. Knapp. 2003. Dominant species maintain ecosystem function with non-
773   random species loss. Ecology Letters.

774 Spiegelhalter, D., N. Best, B. Carlin, and A. van der Linde. 2002. Bayesian measures of model
775   complexity and fit. Journal of the Royal Statistical Society Series B-Statistical Methodology,
776   **64**:583–639.

777 Teller, B. J., P. B. Adler, C. B. Edwards, G. Hooker, and S. P. Ellner. 2016. Linking demography
778   with drivers: climate and competition. Methods in Ecology and Evolution, **7**:171–183.

779 Tilman, D. 1982. Resource competition and community structure. Princeton University Press,
780   Princeton, New Jersey.

781 Yenni, G., P. B. Adler, and S. K. M. Ernest. 2012. Strong self-limitation promotes the persistence
782   of rare species. Ecology, **93**:456–461.

783 Zachmann, L., C. Moffet, and P. B. Adler. 2010. Mapped quadrats in sagebrush steppe: long-term
784   data for analyzing demographic rates and plantplant interactions. Ecology, **91**:3427–3427.

Table 1: Spring soil moisture

|	Model 1	
(Intercept)	8.81*	[5.78; 11.83]
TreatmentDrought	−3.97*	[−4.84; −3.09]
TreatmentIrrigation	3.26*	[2.39; 4.14]
AIC	3191.87	
BIC	3222.92	
Log Likelihood	-1588.93	
Num. obs.	624	
Num. groups: plot	24	
Num. groups: PrecipGroup	8	
Num. groups: date	5	
Var: plot (Intercept)	0.45	
Var: PrecipGroup (Intercept)	0.23	
Var: date (Intercept)	11.24	
Var: Residual	8.90	

* 0 outside the confidence interval
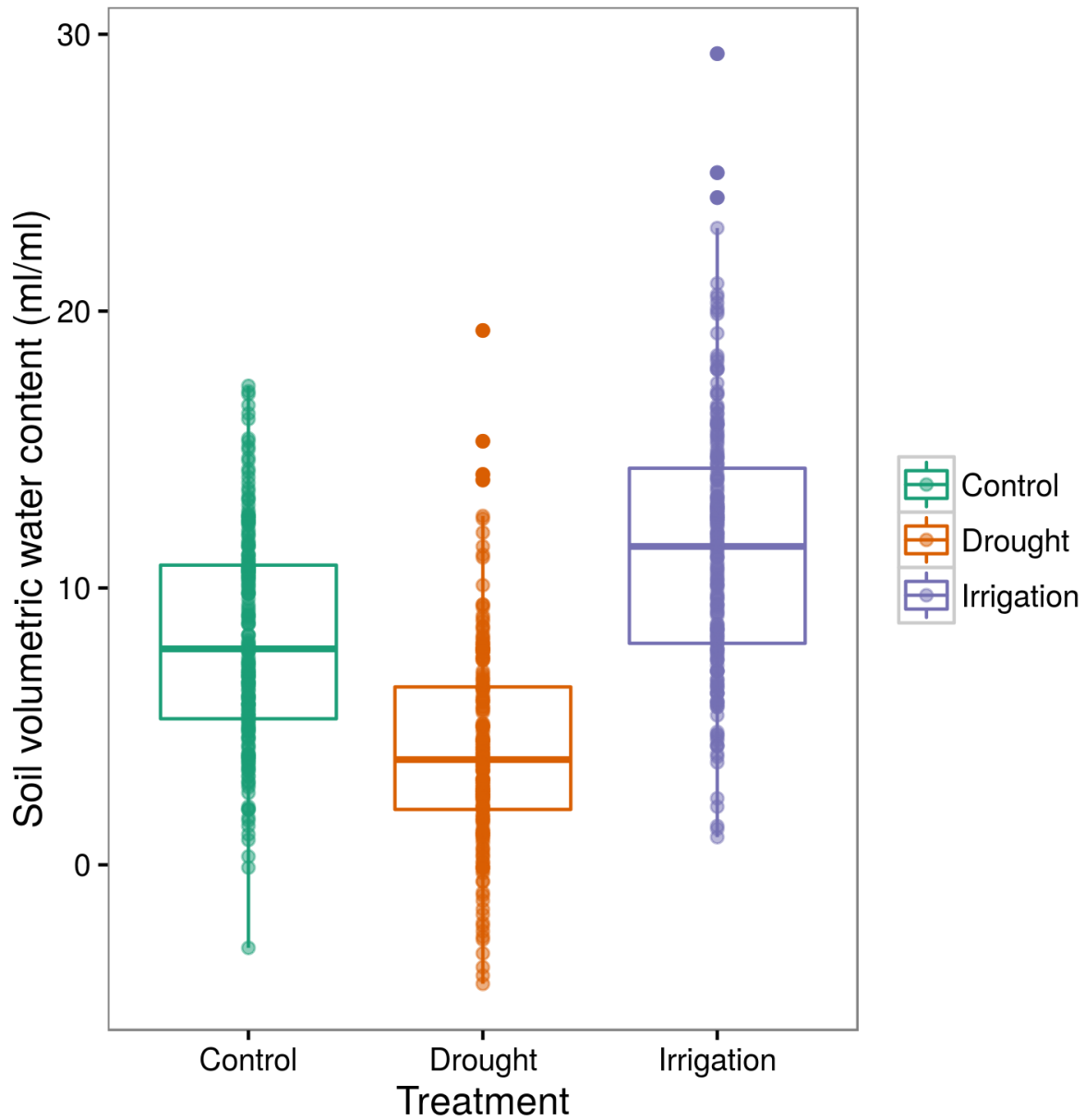
Figure 1: Cover trends by treatment for the four dominant species. Note the difference in y-axis scale between the canopy cover of *A. tripartita* and the basal cover of the dominant grasses. "Shrub removal" refers to removal of *A. tripartita*, and "Grass removal" refers to removal of all perennial grasses. The cover of species in treatments from which they are removed (e.g. *A. tripartita* cover in shrub removal plots) is included to show values at the start of the experiment in 2011 and the efficacy of the removal treatments.
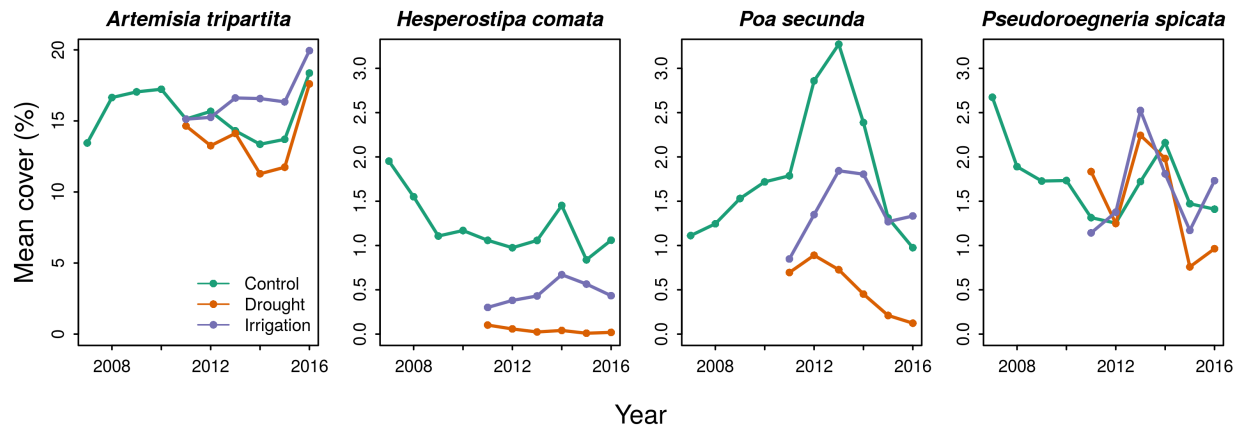
Figure 2: Cover trends by treatment for the four dominant species. Note the difference in y-axis scale between the canopy cover of *A. tripartita* and the basal cover of the dominant grasses. "Shrub removal" refers to removal of *A. tripartita*, and "Grass removal" refers to removal of all perennial grasses. The cover of species in treatments from which they are removed (e.g. *A. tripartita* cover in shrub removal plots) is included to show values at the start of the experiment in 2011 and the efficacy of the removal treatments.

Figure 3: Observed and predicted year-to-year changes in cover for the four dominant species. Mean observed changes (averaged across quadrats) are shown in solid symbols, mean predicted changes are shown in open symbols. Values for control and removal plots are blue and red, respectively. Predictions from the "Baseline" model do account for effects of local species composition on vital rates, but do not include additional effects of removals. Predictions from the "Removal" model include additional treatment effects on vital rates.

Supporting Information

Adler et al., "Weak interspecific interactions"

Supplementary Methods

Interspecific covariance in local crowding

We explored interspecific covariance in local crowding experienced by individual plants, by regressing the W values exerted by one neighbor species, the response variable, against the W values of all other species, the independent variables. Because some $W = 0$, we conducted two separate regressions. First, using all W's, we fitted a generalized linear model with a logit link function to evaluate whether the probability that the focal species' $W = 0$ is influenced by the value of other species' W's. In this model, the dependent variable is a Bernoulli variate coding for the zero or non-zero value of the focal species' crowding, and the independent variables are the W's for all other species. Second, for the set of records in which the focal species has $W > 0$, we performed a linear regression, where the focal species' W is the dependent variable, and the other species' W's are the independent variables. We repeated these regressions for each focal species. Due to large samples size, interspecific W values were often statistically significant predictors of intraspecific. However, they explained very little variance. The maximum reduction in deviance for the generalized linear regressions and R^2 for the linear regressions were both less than 8%. The `R` code for this analysis is included as `..\Wdistrib\exploreSurvivalWs.r`.

Mean field approximation of local crowding for the IPM

Adler et al. (2010) developed a mean field approximation for local crowding when the competition kernels are all Gaussian functions, $F_{jm}(d) = e^{-\alpha_{jm}d^2}$. The approximation is explained in the online SI to Adler et al. (2010) and in section 5.3 of Ellner et al. (2016). Here we explain how that approximation was modified for the IPMs in this paper, which used fitted nonparametric competition kernels.

For $j \neq m$ (between-species competition), overlap between individuals is allowed. The mean field approximation is that from the perspective of any focal plant in species j, individuals of species m are distributed at random in space, independent of each other and of their size.

Consider the region between the circles of radius x and $x + dx$ centered on a focal genet of species j. The area of this annulus is $2\pi x \, dx$ to leading order for $dx \approx 0$. A species m genet in the annulus puts competitive pressure $F_{jm}(x)$ times its area on the focal genet. The expected total competitive pressure from all such genets is therefore is $F_{jm}(x)2\pi x \, dx$ times the expected fractional cover of species m in the annulus (fractional cover is the total area of species m genets, as a fraction of the total area). The excepted fractional cover C_m of species m in the annulus equals its fractional cover in the habitat as a whole, because of the assumption of random distribution spatial distributions. We therefore have $C_m = \int e^u n_m(u,t)du/A$ where A is the total area of the

1

habitat. The total expected competitive pressure on a species-j genet due to species m is then

$$W_{jm} = \int_0^\infty C_m F_{jm}(x) 2\pi x \, dx = C_m \left[2\pi \int_0^\infty x F(x) \, dx \right]. \qquad \text{(SI.1)}$$

The quantity in square brackets is a constant (that is, it only depends on what the kernel function is) so it can be computed once and for all for each kernel used in the IPM. The integral is finite because all fitted kernels fall to zero at a finite distance from the focal plant.

Our kernel fitting method only uses competition kernel values at the "mid-ring" distances halfway between the inner and outer radii of a series of annuli around each focal plant, scaled so that the value at the innermost mid-ring distance equals 1. In the IPM we defined the kernel at other distances by linear interpolation between values at mid-ring distances, except that for the innermost ring a kernel value of 1 was specified at the outer radius of the ring and at distance $x = 0$.

Now consider within-species competition. We assume that conspecifics cannot overlap. Genet shapes are irregular, but we nonetheless implement the no-overlap rule by assuming that a genet of log area u_i is a circle of radius r_i where $\pi r_i^2 = e^{u_i}$. The no-overlap rule is then that the centroids of two conspecific individuals must be separated by at least the sum of their radii.

For any one focal genet, the no-overlap restriction on its neighbors' locations affects only a negligibly small part of the habitat. The expected cover of individuals in the places where they can occur (relative to one focal plant) is thus assumed to equal their expected locations in the habitat as a whole.

Let $C_m(u)$ be the total cover of species m genets of radius r or smaller,

$$C_m(r) = \int_L^{\log(\pi r^2)} e^z n_m(z, t) \, dz. \qquad \text{(SI.2)}$$

A focal genet of radius r cannot have any conspecific neighbors centered at distances less than r. It can have a neighbor centered at distance $x > r$ if that neighbor's radius is no more than $x - r$. Adding up the expected cover of all such possible neighbors for a focal genet of radius r,

$$W_{mm}(r) = 2\pi \int_r^\infty F_{mm}(x) x C_m(x - r) \, dx \qquad \text{(SI.3)}$$

This integral is again finite and computable because the kernels F fall to 0 at finite x.

2

Additional Tables

Table SI-1: Cover change models

Species	ARTR	HECO	POSE	PSSP
(Intercept)	0.00	−0.05	0.01	−0.10
	[−0.41; 0.42]	[−0.21; 0.10]	[−0.26; 0.28]	[−0.28; 0.08]
TreatmentNo_grass	−0.09			
	[−0.75; 0.56]			
TreatmentNo_shrub		0.33*	−0.08	0.21*
		[0.01; 0.65]	[−0.41; 0.25]	[0.01; 0.40]
AIC	284.97	160.41	337.77	253.15
BIC	298.99	172.62	352.65	268.46
Log Likelihood	-137.49	-75.20	-163.88	-121.57
Num. obs.	122	85	145	158
Num. groups: quad	19	11	21	22
Num. groups: year	9	9	9	9
Var: quad (Intercept)	0.43	0.00	0.02	0.00
Var: year (Intercept)	0.00	0.02	0.12	0.06
Var: Residual	0.41	0.32	0.48	0.24

* 0 outside the confidence interval

Table SI-2: Summary of fixed effects for the *A. tripartita* survival model

	mean	sd	0.025quant	0.5quant	0.975quant	mode	kld
(Intercept)	-0.0207	0.2261	-0.4554	-0.0246	0.4367	-0.0321	0.0000
logarea	0.7208	0.0575	0.6109	0.7195	0.8378	0.7171	0.0000
TreatmentNo_grass	-1.3218	0.7343	-2.7293	-1.3340	0.1563	-1.3591	0.0000
W.ARTR	-1.5214	0.2075	-1.9391	-1.5179	-1.1237	-1.5107	0.0000
W.HECO	-0.0694	0.0423	-0.1485	-0.0708	0.0178	-0.0738	0.0000
W.POSE	-0.0049	0.0761	-0.1469	-0.0077	0.1525	-0.0134	0.0000
W.PSSP	0.0281	0.0275	-0.0235	0.0271	0.0849	0.0252	0.0000
W.allcov	-0.0055	0.0083	-0.0219	-0.0054	0.0109	-0.0054	0.0000
W.allpts	0.1694	0.1579	-0.1386	0.1686	0.4812	0.1672	0.0000

Table SI-3: Summary of fixed effects for the *H. comata* survival model

	mean	sd	0.025quant	0.5quant	0.975quant	mode	kld
(Intercept)	1.4189	0.2115	0.9991	1.4190	1.8371	1.4192	0.0000
logarea	1.2885	0.0813	1.1399	1.2843	1.4601	1.2758	0.0000
TreatmentNo_shrub	0.3958	0.4175	-0.4193	0.3942	1.2190	0.3909	0.0000
W.ARTR	-0.0064	0.0028	-0.0120	-0.0064	-0.0009	-0.0064	0.0000
W.HECO	-0.6647	0.0673	-0.7996	-0.6638	-0.5351	-0.6619	0.0000
W.POSE	0.0732	0.0534	-0.0304	0.0728	0.1790	0.0720	0.0000
W.PSSP	0.0190	0.0184	-0.0167	0.0188	0.0554	0.0185	0.0000
W.allcov	0.0021	0.0047	-0.0072	0.0021	0.0113	0.0021	0.0000
W.allpts	-0.1185	0.0919	-0.2998	-0.1183	0.0610	-0.1177	0.0000

Table SI-4: Summary of fixed effects for the *Poa secunda* survival model

	mean	sd	0.025quant	0.5quant	0.975quant	mode	kld
(Intercept)	1.3162	0.1965	0.9242	1.3171	1.7024	1.3186	0.0000
logarea	1.0585	0.0640	0.9365	1.0569	1.1902	1.0537	0.0000
TreatmentNo_shrub	-0.2572	0.1723	-0.5949	-0.2573	0.0811	-0.2576	0.0000
W.ARTR	0.0001	0.0019	-0.0036	0.0001	0.0038	0.0001	0.0000
W.HECO	-0.0153	0.0138	-0.0424	-0.0154	0.0119	-0.0154	0.0000
W.POSE	-1.2632	0.0816	-1.4260	-1.2623	-1.1053	-1.2605	0.0000
W.PSSP	0.0249	0.0122	0.0011	0.0249	0.0490	0.0247	0.0000
W.allcov	-0.0024	0.0026	-0.0075	-0.0024	0.0029	-0.0024	0.0000
W.allpts	0.0018	0.0524	-0.1009	0.0018	0.1048	0.0017	0.0000

Table SI-5: Summary of fixed effects for the *P. spicata* survival model

	mean	sd	0.025quant	0.5quant	0.975quant	mode	kld
(Intercept)	1.2121	0.1699	0.8815	1.2103	1.5533	1.2066	0.0000
logarea	1.5492	0.0976	1.3612	1.5474	1.7473	1.5437	0.0000
TreatmentNo_shrub	-0.1885	0.2208	-0.6237	-0.1879	0.2431	-0.1867	0.0000
W.ARTR	0.0101	0.0021	0.0061	0.0101	0.0142	0.0101	0.0000
W.HECO	0.0046	0.0185	-0.0319	0.0046	0.0406	0.0047	0.0000
W.POSE	0.0245	0.0384	-0.0502	0.0242	0.1007	0.0236	0.0000
W.PSSP	-0.4430	0.0291	-0.5010	-0.4427	-0.3867	-0.4420	0.0000
W.allcov	0.0100	0.0028	0.0046	0.0100	0.0155	0.0100	0.0000
W.allpts	0.0943	0.0605	-0.0246	0.0944	0.2129	0.0944	0.0000

Table SI-6: Summary of fixed effects for the *A. tripartita* growth model

	mean	sd	0.025quant	0.5quant	0.975quant	mode	kld
(Intercept)	0.7378	0.2437	0.2591	0.7378	1.2161	0.7377	0.0000
logarea.t0	0.8663	0.0393	0.7892	0.8663	0.9434	0.8663	0.0000
TreatmentNo_grass	0.1037	0.1436	-0.1783	0.1037	0.3854	0.1037	0.0000
W.ARTR	-0.0364	0.0892	-0.2116	-0.0364	0.1387	-0.0364	0.0000
W.HECO	0.0033	0.0136	-0.0233	0.0033	0.0299	0.0033	0.0000
W.POSE	-0.0573	0.0268	-0.1100	-0.0573	-0.0047	-0.0573	0.0000
W.PSSP	0.0062	0.0084	-0.0102	0.0062	0.0226	0.0062	0.0000
W.allcov	-0.0055	0.0030	-0.0114	-0.0055	0.0004	-0.0055	0.0000
W.allpts	0.0029	0.0477	-0.0908	0.0029	0.0965	0.0029	0.0000

Table SI-7: Summary of fixed effects for the *H. comata* growth model

	mean	sd	0.025quant	0.5quant	0.975quant	mode	kld
(Intercept)	0.3782	0.0797	0.2212	0.3783	0.5343	0.3784	0.0000
logarea.t0	0.8272	0.0205	0.7869	0.8272	0.8674	0.8272	0.0000
TreatmentNo_shrub	-0.0162	0.1336	-0.2785	-0.0162	0.2460	-0.0162	0.0000
W.ARTR	-0.0031	0.0010	-0.0051	-0.0031	-0.0010	-0.0031	0.0000
W.HECO	-0.0479	0.0195	-0.0862	-0.0479	-0.0098	-0.0479	0.0000
W.POSE	0.0242	0.0162	-0.0077	0.0242	0.0560	0.0242	0.0000
W.PSSP	-0.0151	0.0065	-0.0279	-0.0151	-0.0023	-0.0151	0.0000
W.allcov	-0.0038	0.0019	-0.0076	-0.0038	0.0000	-0.0038	0.0000
W.allpts	-0.0513	0.0380	-0.1258	-0.0513	0.0232	-0.0513	0.0000

Table SI-8: Summary of fixed effects for the *Poa secunda* growth model

	mean	sd	0.025quant	0.5quant	0.975quant	mode	kld
(Intercept)	0.4923	0.0681	0.3581	0.4923	0.6259	0.4924	0.0000
logarea.t0	0.6750	0.0232	0.6292	0.6750	0.7203	0.6751	0.0000
TreatmentNo_shrub	0.2161	0.0644	0.0897	0.2161	0.3425	0.2161	0.0000
W.ARTR	-0.0002	0.0008	-0.0019	-0.0002	0.0014	-0.0002	0.0000
W.HECO	0.0039	0.0063	-0.0084	0.0039	0.0161	0.0039	0.0000
W.POSE	-0.2641	0.0387	-0.3400	-0.2641	-0.1883	-0.2641	0.0000
W.PSSP	-0.0073	0.0056	-0.0183	-0.0073	0.0038	-0.0073	0.0000
W.allcov	-0.0003	0.0012	-0.0026	-0.0003	0.0020	-0.0003	0.0000
W.allpts	-0.0254	0.0231	-0.0709	-0.0254	0.0200	-0.0254	0.0000

Table SI-9: Summary of fixed effects for the *P. spicata* growth model

	mean	sd	0.025quant	0.5quant	0.975quant	mode	kld
(Intercept)	0.3987	0.0660	0.2690	0.3987	0.5281	0.3988	0.0000
logarea.t0	0.8249	0.0149	0.7956	0.8249	0.8543	0.8249	0.0000
TreatmentNo_shrub	0.1948	0.0714	0.0546	0.1948	0.3349	0.1948	0.0000
W.ARTR	-0.0025	0.0008	-0.0041	-0.0025	-0.0010	-0.0025	0.0000
W.HECO	-0.0118	0.0072	-0.0260	-0.0118	0.0023	-0.0118	0.0000
W.POSE	-0.0067	0.0130	-0.0323	-0.0067	0.0189	-0.0067	0.0000
W.PSSP	-0.1480	0.0133	-0.1740	-0.1480	-0.1220	-0.1480	0.0000
W.allcov	-0.0036	0.0011	-0.0057	-0.0036	-0.0015	-0.0036	0.0000
W.allpts	-0.0522	0.0236	-0.0984	-0.0522	-0.0060	-0.0522	0.0000

Table SI-10: *Poa secunda* growth with *Artemisia* canopy effect

	Model 1
(Intercept)	0.49*
	[0.36; 0.62]
logarea.t0	0.68*
	[0.63; 0.72]
TreatmentNo_shrub	0.24*
	[0.09; 0.38]
W.ARTR	−0.00
	[−0.00; 0.00]
W.HECO	0.00
	[−0.01; 0.02]
W.POSE	−0.26*
	[−0.34; −0.19]
W.PSSP	−0.01
	[−0.02; 0.00]
W.allcov	−0.00
	[−0.00; 0.00]
W.allpts	−0.02
	[−0.07; 0.02]
inARTR	−0.06
	[−0.28; 0.16]
AIC	15641.80
BIC	15734.29
Log Likelihood	-7806.90
Num. obs.	5469
Num. groups: year	31
Var: year (Intercept)	0.11
Var: year logarea.t0	0.01
Cov: year (Intercept) logarea.t0	-0.02
Var: Residual	0.98

* 0 outside the confidence interval

Table SI-11: *P. spicata* growth with *Artemisia* canopy effect

	Model 1
(Intercept)	0.42*
	[0.29; 0.56]
logarea.t0	0.82*
	[0.79; 0.86]
TreatmentNo_shrub	0.24*
	[0.09; 0.40]
W.ARTR	−0.00*
	[−0.00; −0.00]
W.HECO	−0.01*
	[−0.03; −0.00]
W.POSE	−0.01
	[−0.03; 0.02]
W.PSSP	−0.14*
	[−0.16; −0.11]
W.allcov	−0.00*
	[−0.01; −0.00]
W.allpts	−0.06*
	[−0.10; −0.01]
inARTR	−0.14
	[−0.35; 0.08]
AIC	15282.37
BIC	15376.25
Log Likelihood	-7627.18
Num. obs.	6039
Num. groups: year	31
Var: year (Intercept)	0.12
Var: year logarea.t0	0.01
Cov: year (Intercept) logarea.t0	-0.03
Var: Residual	0.71

* 0 outside the confidence interval

7

Table SI-12: *Poa secunda* growth with year-by-treatment interaction

	Model 1
(Intercept)	0.49*
	[0.37; 0.62]
trtYears1	0.06
	[−0.17; 0.29]
trtYears2	0.24
	[−0.01; 0.49]
trtYears3	0.23
	[−0.05; 0.51]
trtYears4	0.25
	[−0.07; 0.56]
trtYears5	0.45*
	[0.11; 0.79]
logarea.t0	0.68*
	[0.63; 0.72]
W.ARTR	−0.00
	[−0.00; 0.00]
W.HECO	0.00
	[−0.01; 0.02]
W.POSE	−0.26*
	[−0.34; −0.19]
W.PSSP	−0.01
	[−0.02; 0.00]
W.allcov	−0.00
	[−0.00; 0.00]
W.allpts	−0.03
	[−0.07; 0.02]
AIC	15648.62
BIC	15760.94
Log Likelihood	-7807.31
Num. obs.	5469
Num. groups: year	31
Var: year (Intercept)	0.11
Var: year logarea.t0	0.01
Cov: year (Intercept) logarea.t0	-0.02
Var: Residual	0.98

* 0 outside the confidence interval

Table SI-13: *P. spicata* growth with year-by-treatment interaction

	Model 1
(Intercept)	0.42*
	[0.28; 0.55]
trtYears1	0.26
	[−0.01; 0.54]
trtYears2	−0.05
	[−0.32; 0.22]
trtYears3	0.44*
	[0.14; 0.73]
trtYears4	0.42*
	[0.12; 0.72]
trtYears5	−0.11
	[−0.42; 0.20]
logarea.t0	0.82*
	[0.79; 0.86]
W.ARTR	−0.00*
	[−0.00; −0.00]
W.HECO	−0.01*
	[−0.03; −0.00]
W.POSE	−0.01
	[−0.03; 0.02]
W.PSSP	−0.14*
	[−0.16; −0.11]
W.allcov	−0.00*
	[−0.01; −0.00]
W.allpts	−0.06*
	[−0.10; −0.01]
AIC	15281.67
BIC	15395.67
Log Likelihood	-7623.83
Num. obs.	6039
Num. groups: year	31
Var: year (Intercept)	0.12
Var: year logarea.t0	0.01
Cov: year (Intercept) logarea.t0	-0.03
Var: Residual	0.71

* 0 outside the confidence interval

Table SI-14: Summary of fixed effects for the recruitment model (symbols correspond to Eqns. 10 and 11)

	mean	sd	X2.5.	X97.5.	Rhat	n.eff
$\gamma[1]$	0.3341	0.7071	-1.1262	1.6391	1.0018	1100
$\gamma[2]$	3.4488	0.4468	2.5010	4.3401	1.0904	25
$\gamma[3]$	3.2440	0.3650	2.4840	3.9190	1.0536	34
$\gamma[4]$	2.9054	0.3689	2.1820	3.6160	1.0149	110
$\chi[2,2]$	-0.0953	0.4093	-0.8854	0.7570	1.0010	2000
$\chi[2,3]$	-1.2787	0.3325	-1.9370	-0.6392	1.0041	420
$\chi[2,4]$	0.0951	0.2617	-0.4121	0.6063	1.0023	810
$\chi[3,1]$	-1.4366	0.8544	-3.1491	0.1132	1.0006	2000
$\omega[1,1]$	-0.5881	0.1018	-0.7639	-0.3720	1.0197	82
$\omega[1,2]$	0.0635	0.0651	-0.0528	0.1997	1.0329	59
$\omega[1,3]$	0.0220	0.0422	-0.0610	0.1040	1.0036	920
$\omega[1,4]$	0.1164	0.0456	0.0347	0.2123	1.0197	96
$\omega[2,1]$	-0.4800	0.1522	-0.7746	-0.1906	1.0029	2000
$\omega[2,2]$	-1.7368	0.1297	-1.9841	-1.4819	1.0006	2000
$\omega[2,3]$	0.0388	0.0865	-0.1287	0.2138	1.0152	100
$\omega[2,4]$	-0.3682	0.0926	-0.5434	-0.1881	1.0005	2000
$\omega[3,1]$	-0.6589	0.3342	-1.3131	-0.0155	1.0096	280
$\omega[3,2]$	-0.1021	0.1981	-0.4828	0.2936	1.0089	210
$\omega[3,3]$	-1.8943	0.1611	-2.2060	-1.5850	1.0084	2000
$\omega[3,4]$	-0.1953	0.1508	-0.4968	0.0995	1.0074	2000
$\omega[4,1]$	-0.1867	0.3000	-0.7608	0.4486	1.0099	190
$\omega[4,2]$	-0.3746	0.1896	-0.7224	-0.0115	1.0453	55
$\omega[4,3]$	0.1131	0.1437	-0.1583	0.4170	1.0321	55
$\omega[4,4]$	-1.7379	0.1549	-2.0400	-1.4409	1.0116	1400
$\theta[1]$	0.6198	0.0740	0.4835	0.7766	1.0008	2000
$\theta[2]$	1.1197	0.1428	0.8666	1.4450	1.0008	2000
$\theta[3]$	1.1718	0.1068	0.9685	1.3890	1.0008	2000
$\theta[4]$	1.0961	0.1060	0.9009	1.3280	1.0022	890
$p[1]$	0.8137	0.1228	0.4813	0.9525	1.0399	60
$p[2]$	0.9996	0.0005	0.9984	1.0000	1.0007	2000
$p[3]$	0.7906	0.1288	0.4273	0.9382	1.0176	2000
$p[4]$	0.7502	0.1480	0.3920	0.9453	1.0150	2000

Additional Figures